

Frequency dependent elastic properties and attenuation in heavy-oil sands: comparison between measured and modeled data

Agnibha Das*, and Michael Batzle, Colorado School of Mines

SUMMARY

We have measured elastic (bulk and shear modulus) and acoustic (compressional and shear wave velocities) properties of heavy-oil sands over a range of frequencies (2 – 2000Hz) covering the seismic bandwidth and at ultrasonic frequencies (0.8MHz). The measurements were carried on heavy-oil sand sample from Asphalt Ridge, Utah at a constant temperature (20°C) and different confining pressures using the low frequency experimental setup at Colorado School of Mines. Four different modes of intrinsic attenuation, extensional (Q_E^{-1}), shear-wave (Q_S^{-1}), compressional-wave (Q_P^{-1}) and bulk compressibility (Q_K^{-1}) were estimated. Both compressional and shear wave velocities show significant dispersion probably due to both the the inherent viscoelastic property of heavy oil and viscoelasticity arising due to oil and sand interactions. The measured attenuation (Q^{-1}) values are significantly high indicating significant loss of energy during wave propagation. We made an attempt to model the measured acoustic properties using effective medium theories. The results show reasonably good agreement between the measured data and modeled response especially at non-zero confining pressures. The measured attenuations were modeled using the Cole-Cole model.

INTRODUCTION

Heavy-oil sands are an important unconventional energy resource. The total inplace volume of heavy-oil is much larger than that of conventional light oil. Current methods of production from heavy-oil reservoirs are dominated by thermal techniques such as in-situ combustion, THAI (Toe to Heel Air Injection) and SAGD (Steam Assisted Gravity Drainage). Acoustic Impedance (AI) difference maps are extensively used for quantitative seismic monitoring of heavy-oil reservoirs undergoing production. Correct understanding of the rock physics of heavy-oil and heavy-oil sands is important for interpreting the AI difference maps in terms of temperature, fluid property and fluid saturation changes. Heavy-oil can exist in three different phases: solid, liquid and quasi-solid (Han et al., 2009). In the quasi-solid state heavy oils have a non-negligible shear modulus that is highly temperature and frequency dependent. Laboratory measured data over a range of frequencies are important for developing our understanding of the frequency dependent behavior of heavy-oil and heavy-oil sands. Over the last few years laboratory measured elastic properties of heavy-oil and heavy-oil sands have been published by a number of researchers (Han et al., 2009, 2008, 2007; Behura et al., 2007). However, most of the published data has been measured either at ultrasonic frequencies or over a limited range of frequencies only.

We have measured bulk modulus (K), shear modulus (μ), p -wave velocities and s -wave velocities for a heavy oil sand sam-

ple from Asphalt Ridge, Utah over a wide frequency band that covers the seismic bandwidth and ultrasonics. The measurements were done both as a function of frequency and confining pressure. The studied sample comprises of unconsolidated quartz grains held together only by viscous heavy-oil. Figure 1 shows the SEM image of a heavy-oil sand. The porosity of the sands are approximately 36% and the permeability is also very high. Oil saturation in the sands lie between 85 – 90%. The remaining 10 – 15% of the porosity is filled water, but, since the sample comes from an outcrop most of that is expected to have dried out.

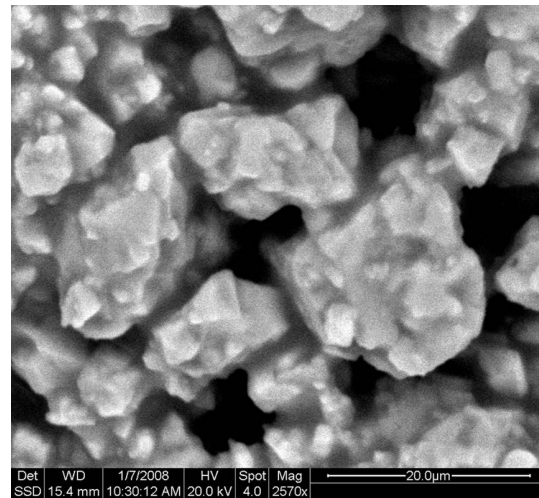


Figure 1: SEM image of heavy oil sand. The black areas indicate voids and the white areas indicate clusters of sand and heavy oil. Note the high porosity of the sample.

We have also modeled the elastic properties of this heavy-oil sand using a combined effective medium approach (Das and Batzle, 2009; Hornby et al., 1994; Sheng, 1991) and compared with our measured data. The match between the two is reasonably good. Along with the elastic property we also measured intrinsic attenuation in the rock. Modulus dispersion and attenuation was then modeled using the Cole-Cole equations (Cole and Cole, 1941).

EXPERIMENTAL PROCEDURE

We conducted a stress-strain experiment in conjunction with pulse transmission to measure elastic properties of the heavy-oil sand mentioned in the previous section at frequencies between 2Hz and 0.8MHz. In the experiment a fixed frequency sinusoidal stress is applied to the rock sample and the resultant sinusoidal strain is measured from the strain gages that are attached to the surface of the sample. We assumed that our rock sample is isotropic so we needed only two parameters,

Elastic properties and attenuation in heavy oil sands

Young's modulus (E) and Poisson's ratio (ν) to fully characterize the rock in terms of its elastic property. We needed only two sets of strain gages on the sample surface, one perpendicular to the stress direction and the other parallel to it for estimating these two parameters. The recorded strains amplitudes are comparable to seismic strain amplitudes. The details of the experimental setup and sample preparation is given in (Batzle et al., 2006). We measured the rock properties at three different confining pressures: 0MPa , 3.45MPa and 6.89MPa , simulating subsurface conditions. Since, this type of heavy-oil sand generally occurs at shallow depths ($< 1200\text{ft}$), the selected pressures are quite reasonable. The sample also has pore fluid lines at both ends and wire mesh screens on the sides. So, we could monitor pore pressures in the sample which was not observed to change in response to changing confining pressures. Hence, the differential pressure is equal to the confining pressure in our experiment.

Observations

Figure 2 and Figure 3 show the measured p -wave velocity (V_p) and s -wave velocity (V_s) respectively as functions of log frequency.

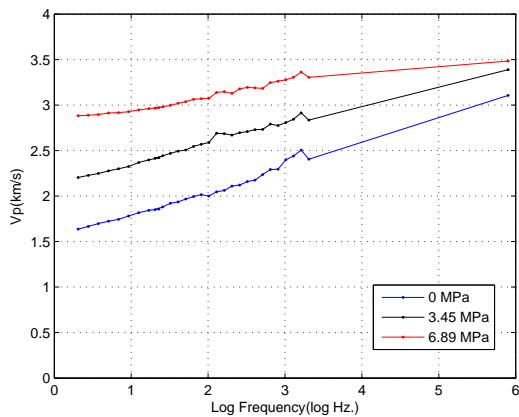


Figure 2: Measured V_p Vs. Log Frequency for different pressures.

Both V_p and V_s show significant amount of dispersion within the seismic bandwidth and the ultrasonic velocity is higher than seismic velocities. Heavy-oils are viscoelastic so at low frequencies the long chain molecules in them have time to come to equilibrium resulting in a lower effective modulus and lower velocities. At higher frequencies the long chain molecules get entangled and do not have sufficient time to relax resulting in a higher effective modulus and higher velocities. However, this is under the assumption that viscous losses in heavy-oil is the only dominant mechanism of energy loss in heavy-oil saturated rocks as pointed out by Behura et al. (2007). The increase in velocities with increasing pressure is due to increase in the overall stiffness of the rock as a result of closing down of compliant pores/cracks.

Modeling

We used the combined effective medium approach to model the viscoelastic properties of the heavy-oil sand. A similar ap-

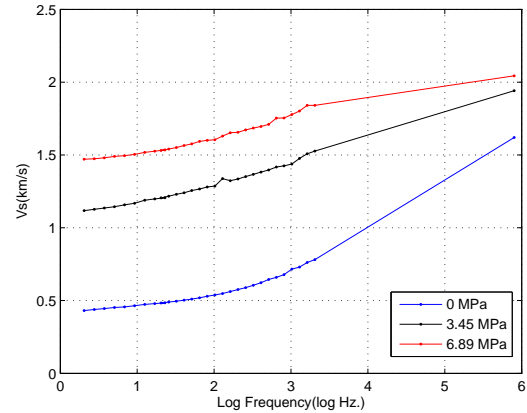


Figure 3: Measured V_s Vs. Log Frequency for different pressures.

proach was used by the authors to model the viscoelastic properties of the heavy oil saturated Uvalde carbonate rock (Das and Batzle, 2009). As explained in Das and Batzle (2009) the combined effective medium approach creates a biconnected medium in which both solid and fluid phases form interconnected networks, a micro-geometry that is typical of sedimentary rocks and also observable in our heavy oil sand sample (Figure 1). Also, the effective medium created by this approach both supports shear and conducts electricity. In the current study however we have not considered the electro-static problem. The other reason for using the effective medium calculations is that Gassmann's equation (Gassmann, 1951) and the generalized Gassmann's equation (Ciz and Shapiro, 2007) may not be applicable in heavy-oil sand reservoirs due to both the non-negligible shear modulus of heavy-oil and the possibility that the dry rock properties of unconsolidated rocks such as heavy-oil sands might change with changing oil properties and/or saturation.

Figure 4 and Figure 5 show the comparison between modeled and measured moduli and velocities.

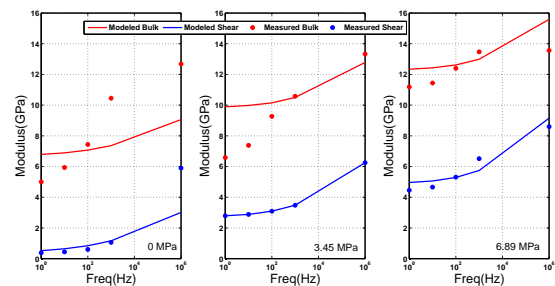


Figure 4: Measured and modeled moduli for different pressures.

For our models we have used frequency dependent shear modulus of the heavy-oil from FLAG09 and did not consider any viscoelastic behavior of the rock matrix. Hence, viscoelastic-

Elastic properties and attenuation in heavy oil sands

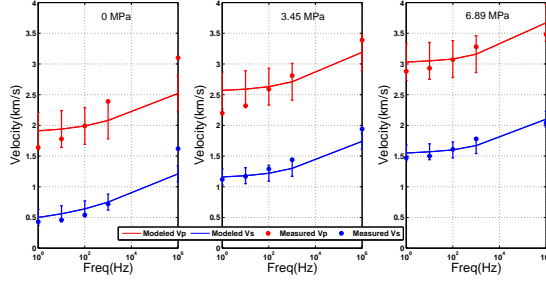


Figure 5: Measured and modeled velocities for different pressures. Errorbars indicate one standard deviation on either side of the modeled response

ity of the effective properties is due to that of oil only. We considered a dual porosity model where the total porosity is divided into stiff pores with large aspect ratios (0.3) and soft pores with low aspect ratios (0.07). For modeling the higher pressure data we reduced the volume of soft/compliant pores at each pressure step and an equivalent amount was reduced from the total porosity. This is consistent with the fact that with increasing differential pressure the compliant pores close resulting in making the rock stiffer. Shear modulus predictions are better than bulk modulus predictions when compared to measured data (Figure 4). The discrepancies are less at higher pressures. The measured data and modeled response have different dispersion trends which indicates that viscous losses in the oil may not be the only attenuation mechanism in the rock. The ‘squishing’ of the grain-fluid aggregate could be a possible attenuation mechanism at intermediate frequencies affecting overall bulk compressibilities. This is quite different from squirt flow (Mavko and Jizba, 1991) which can be safely ruled out as a possible attenuation mechanism due to the immobility of the oil (Behura et al., 2007). With increasing pressures the unconsolidated heavy oil sands get compacted which greatly reduces ‘squishing’ of the grain-fluid aggregate and viscous losses in the oil again dominate as the primary attenuation mechanism and this explains the lower observed discrepancies at higher pressures. The match between modeled response and measured data for velocities is much better than that for modulus (Figure 5). Most of the measured data points fall within one standard deviation of the modeled response.

ATTENUATION

Intrinsic attenuation in the heavy oil rock was measured from the phase lag between the stress and the strain wave in our low frequency stress-strain experiment. Intrinsic attenuation can be described as the inverse of the quality factor, Q . Q^{-1} is the ratio of the imaginary (loss component) and real (storage component) parts of the complex modulus of viscoelastic materials. Q^{-1} is also equal to $\tan \theta$, where θ is the phase lag between the stress and strain waves. In our experiments we estimated four different modes of intrinsic attenuation, extensional (Q_E^{-1}), shear-wave (Q_S^{-1}), compressional-wave (Q_P^{-1}) and bulk compressibility (Q_K^{-1}). Out of these four only Q_E^{-1}

can be directly measured from the phase lag between the Aluminium standard strain and the strain from the gage that is placed perpendicular to the stress direction. The remaining three are estimated from the following equations (White, 1965; Winkler and Nur, 1982).

$$\frac{1}{Q_S} \approx \frac{1}{Q_E} - \frac{\nu \tan \theta_\nu}{1 + \nu} \quad (1)$$

$$\frac{(1 - \nu)(1 - 2\nu)}{Q_P} = \frac{1 + \nu}{Q_E} - \frac{2\nu(2 - \nu)}{Q_S} \quad (2)$$

$$\frac{1 - 2\nu}{Q_K} = \frac{3}{Q_E} - \frac{2(\nu + 1)}{Q_S} \quad (3)$$

where, ν is the Poisson’s ratio and θ_ν is the phase lag between the vertical and horizontal strains. Figure 6 shows the four different attenuation modes as a function of frequency at 6.89 MPa differential pressure. We have not calculated Q^{-1} for ultrasonic frequency, but it can be done using the spectral ratio method (Toksoz et al., 1979).

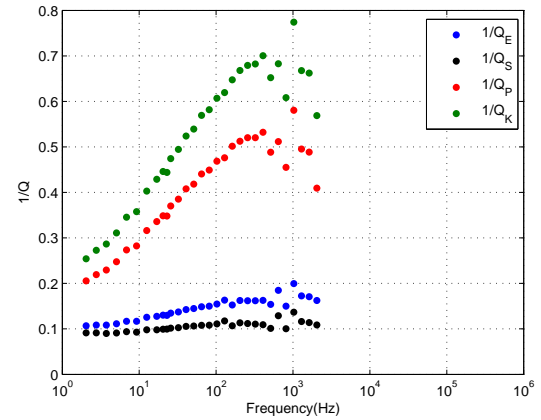


Figure 6: $1/Q$ vs. frequency at 6.89 MPa differential pressure

The relationship between the different attenuation modes from Figure 6 is :

$$Q_K^{-1} > Q_P^{-1} > Q_E^{-1} > Q_S^{-1} \quad (4)$$

which is typical of partially saturated rocks (Winkler and Nur, 1982). Peak attenuation occurs at approximately 407Hz which indicates that the maximum loss of energy occurs at this frequency during a cycle of loading. We used the Cole-Cole model (Cole and Cole, 1941) to predict attenuation from the observed dispersion in the measured modulus. The Cole-Cole equation is an empirical relationship between the complex modulus, the ‘zero’ and ‘infinite’ frequency modulus and relaxation time, and is given as :

$$M^*(\omega) = \frac{M_0 - M_\infty}{1 + (i\omega\tau_0)^{(1-\alpha)}} + M_\infty \quad (5)$$

Elastic properties and attenuation in heavy oil sands

where, M^* is the complex modulus, M_0 is the zero frequency modulus, M_∞ is the infinite frequency modulus, τ_0 is the relaxation time defined as the ratio between the dynamic viscosity and the infinite frequency modulus and α is the parameter that controls the width of the distribution of relaxation times. Figures 7 and 8 shows the Cole-Cole fit to the measured shear modulus and the corresponding Q_S^{-1} calculations using Cole-Cole model compared with measured Q_S^{-1} at two different pressures. The modeled and measured attenuation values start to share the trend as pressure on the rocks are increased.

Observation

The measured attenuation and the results obtained from Cole-Cole modeling suggest that viscous losses in the heavy-oil is the predominant mechanism for energy loss in heavy-oil sands. This is consistent with observations made by Behura et al. (2007). There may be some contribution from the ‘squishing’ of grain and oil aggregates especially at low differential pressures, but, that seems to diminish at higher differential pressures when viscous losses dominate. The observed and modeled high attenuation values suggest that there would be significant energy losses in the rock when an acoustic wave propagates through it. It is extremely important to keep this in mind when doing time lapse studies.

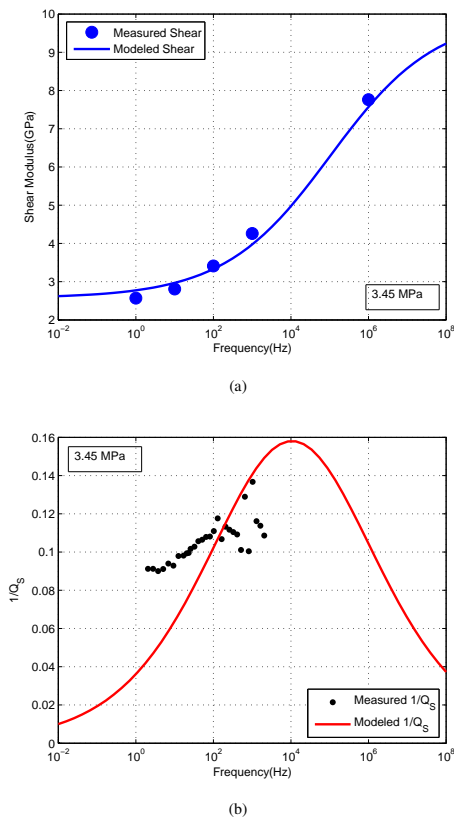


Figure 7: Measured and modeled (a) shear modulus and (b) Q_S^{-1} for the heavy oil sands using the Cole-Cole model at 3.45 MPa differential pressure.

CONCLUSIONS

We have presented elastic and acoustic properties of the Asphalt Ridge heavy oil sand measured over a wide range of frequencies that covers the seismic bandwidth and ultra-sonics. A reasonably good match was obtained between the measured velocities and velocities predicted using the combined effective medium approach. This is important to know because now this approach can be used to predict the properties of rocks in both consolidated and unconsolidated heavy-oil saturated rocks. Attenuation measurements and Cole-Cole calculations show that the viscoelasticity of heavy oil is the main contributor to the overall viscoelasticity of the heavy-oil sand. However, at low differential pressures effect of other potential loss mechanisms can also be present. These mechanisms seem to disappear at high differential pressures.

ACKNOWLEDGEMENT

This work was sponsored by the Fluids and DHI consortium of the Colorado School of Mines and University of Houston.

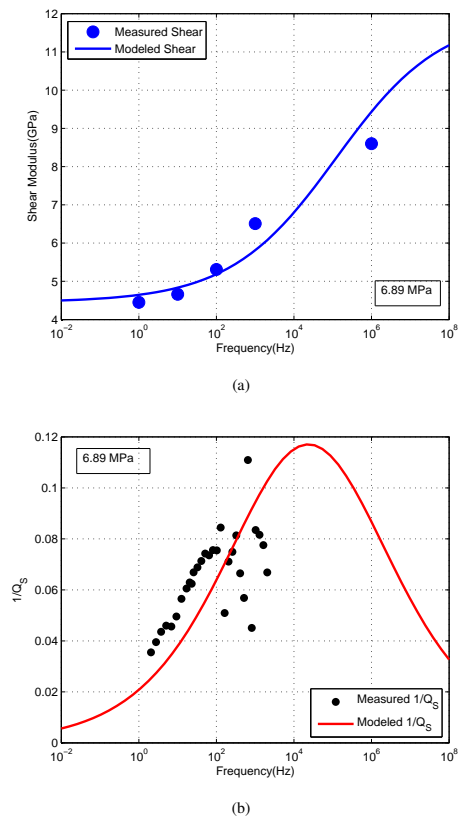


Figure 8: Measured and modeled (a) shear modulus and (b) Q_S^{-1} for the heavy oil sands using the Cole-Cole model at 6.89 MPa differential pressure.

Elastic properties and attenuation in heavy oil sands

REFERENCES

- Batzle, M., D. H. Han, and R. Hofmann, 2006, Fluid mobility and frequency-dependent seismic measurements - direct measurements: *Geophysics*, **71**, N1–N9.
- Behura, J., M. Batzle, R. Hofmann, and J. Dorgan, 2007, Heavy oils: Their shear story: *Geophysics*, **72**, E175–E183.
- Ciz, R. and S. A. Shapiro, 2007, Generalization of gassmann equations for porous media saturated with a solid material: *Geophysics*, **72**, A75–A79.
- Cole, K. S. and R. H. Cole, 1941, Dispersion and absorption in dielectrics: *Journal of chemical physics*, **9**, 341–351.
- Das, A. and M. Batzle, 2009, A combined effective medium approach for modeling the viscoelastic properties of heavy oil reservoirs: 79th Annual International Meeting, Expanded Abstracts, 1589–1593.
- Gassmann, F., 1951, Über die elastizität poroser medienl: *Der Natur Gesellschaft*, **96**, 1–23.
- Han, D. H., H.Z. Zhao, Q. Yao, and M. Batzle, 2007, Velocity of heavy-oil sand: 77th Annual International Meeting, Expanded Abstracts, **27**, 1619–1623.
- Han, D. H., J. Liu, and M. Batzle, 2008, Seismic properties of heavy oils-measured data: *The Leading Edge*, **27**, 1108–1115.
- , 2009, Viscosity model of heavy oil with calibration of shear velocity data: 79th Annual International Meeting, Expanded Abstracts, 2115–2119.
- Hornby, B. E., L. M. Schwartz, and J. A. Hudson, 1994, Anisotropic effective medium modeling of the elastic properties of shales: *Geophysics*, **59**, 1570–1583.
- Mavko, G. and D. Jizba, 1991, Estimating grain-scale fluid effects on velocity dispersion in rocks: *Geophysics*, **56**, 1940–1949.
- Sheng, P., 1991, Consistent modeling of the electrical and elastic properties of sedimentary rocks: *Geophysics*, **56**, 1236–1243.
- Toksoz, M. N., D. H. Johnson, and A. Timur, 1979, Attenuation of seismic waves in dry and saturated rocks: I. laboratory measurements: *Geophysics*, **44**, 681–690.
- White, J. E., 1965, *Seismic waves: radiation, transmission, and attenuation*: McGraw-Hill, New York.
- Winkler, K. W. and A. Nur, 1982, Seismic attenuation: Effects of pore fluids and frictional-sliding: *Geophysics*, **47**, 1–15.